frontiers | Frontiers in Sustainable Food Systems

TYPE Original Research
PUBLISHED 10 July 2025
DOI 10.3389/fsufs.2025.1591966



OPEN ACCESS

EDITED BY
Catherine Nkirote Kunyanga,
University of Nairobi, Kenya

REVIEWED BY
Sen Cao,
Guiyang University, China
Guangheng Wu,
Wuyi University, China

*CORRESPONDENCE
Wen Yang
✉ yangwen3409@126.com
Zhiwei Lei
✉ leizhiwei816@163.com

RECEIVED 11 March 2025
ACCEPTED 21 May 2025
PUBLISHED 10 July 2025

CITATION
Liu H, Yao J, Yin R, Ma C, Li L, Yang W and Lei Z (2025) Antifungal mechanism of carvacrol and osthole can disrupt cell structure integrity and interfere with energy metabolism in *Neopestalotiopsis ellipsospora*. *Front. Sustain. Food Syst.* 9:1591966. doi: 10.3389/fsufs.2025.1591966



# Antifungal mechanism of carvacrol and osthole can disrupt cell structure integrity and interfere with energy metabolism in *Neopestalotiopsis ellipsospora*

Huifang Liu, Jianmei Yao, Rongxiu Yin, Chiyu Ma, Lulu Li, Wen Yang* and Zhiwei Lei*

Guizhou Tea Research Institute, Guizhou Academy of Agricultural Sciences, Guiyang, China

**Introduction:** Tea gray blight disease is a major leaf disease in tea plants, significantly reducing tea quality and yield. Plants are rich in bioactive compounds that are safe, non-toxic, and biodegradable. In this study, we evaluated the antifungal activities and mechanisms of 11 plant extracts against *N. ellipsospora*.

**Methods:** This study evaluated the antifungal activity of 11 plant extracts against *N. ellipsospora* of tea gray blight disease and systematically examined the impacts of osthole and carvacrol on the mycelial morphology, mycelial weight, cell microstructure, membrane permeability, various biochemical substrate levels and related gene expression levels of *N. ellipsospora*.

**Results:** The results showed that carvacrol and osthole exhibited significant antifungal effects among 11 plant extracts with $EC_{50}$ values of 24.40 and 9.38 mg/L, respectively. Further research demonstrated that carvacrol and osthole significantly inhibited mycelial growth, reduced lesion areas on tea leaves, and markedly affected mycelial morphology and ultrastructure. Observations of mycelial morphology and ultrastructure revealed that carvacrol and osthole caused shrinkage and distortion of the mycelial surface, damage to cell wall and membrane, and disorganization of cellular organelles. Particularly carvacrol and osthole significantly increased chitinase activity, inhibited $\beta$-1,3-glucanase activity, and regulated the expression of genes encoding these enzymes.

**Discussion:** The findings indicated that carvacrol and osthole could inhibit the growth of *N. ellipsospora* by disrupting the integrity of the cell wall and membrane and interfere with energy metabolism. This study would provide a theoretical basis for the development of novel plant-based fungicides.

KEYWORDS

***Neopestalotiopsis ellipsospora*, carvacrol, osthole, antifungal activity, biochemical mechanism**

## 1 Introduction

Tea (Zhao et al., 2019) (*Camellia sinensis* (L.) Kuntze) is rich in substances such as tea polyphenols, alkaloids, proteins, amino acids, and vitamins, and has effects such as antioxidation, anti-inflammation, blood pressure reduction, anti-aging, and weight loss (Cui et al., 2024; Jiang et al., 2020; Luo et al., 2023), and is widely loved by people around the world. However, due to the botanical characteristics of tea plants that prefer

shade and humidity, tea plants are often infected by different plant pathogens during the cultivation process, resulting in serious economic losses (Chen et al., 2019; Pandey et al., 2021; Yuan et al., 2019). Especially, tea gray blight disease (Saleh et al., 2021) is one of the most common leaf diseases in tea cultivation, caused by pathogens of genera *Pestalotiopsis* (Zhang J. et al., 2024), *Pseudopestalotiopsis* (Zheng et al., 2021), and *Neopestalotiopsis* (Wang et al., 2022). Infected tea leaves form irregular ring-shaped lesions, and this disease can cause a large number of tea leaves to fall off in severe cases (Murugavel et al., 2024; Xu et al., 2023). This disease occurs in many countries such as China, India, Sri Lanka, and Japan. Currently, the prevention and control of tea gray blight disease is still highly dependent on chemical control (Sanjay et al., 2008) methods in China. However, unreasonable use of chemical pesticides has seriously threatened the quality and safety of agricultural products (Chattopadhyay et al., 2017; Chu et al., 2022; Garvey, 2022) and the stability of the agricultural ecological environment (Sen et al., 2020; Zhou and Li, 2021) and cannot be ignored. Therefore, it is important to develop a safe and effective method to control tea gray blight disease.

In recent years, numerous research findings have shown that various plant extracts exhibit promising potential in combating agricultural pathogens (Al-Otibi et al., 2023; Cui et al., 2019; Lee et al., 2022; Nair and van Staden, 2017), offering new directions and hopes for resolving the numerous drawbacks brought about by chemical control methods. They are expected to become effective alternative solutions for prevention and control of agricultural diseases in the future, and their related research and applications have been increasingly attracting extensive attention and emphasis (Ma et al., 2016). The extracts from plants such as *Magnolia officinalis* (Jiying et al., 2024; Zhang Y. et al., 2024), *Cymbopogon citratus* (Sawadogo et al., 2022), *Tamarix aphylla* (Alshehri et al., 2022), *Momordica charantia* seed (Chen et al., 2023; Ramalingam et al., 2020), *Argemone ochroleuca* (Nezelo et al., 2024), and *Adenophyllum porophyllum* (Aguilar-Rodríguez et al., 2022; Hernández-Ceja et al., 2021) have possessed relatively good antifungal activities. Studies have identified and isolated several plant-derived antifungal compounds, such as magnolol, honokiol (Bang et al., 2000), osthole (Hu et al., 2023), citronellol (Zhang J. et al., 2024), citronellal (Zhou et al., 2022), eugenol (Marchese et al., 2017), and citral (Luo et al., 2024), which exhibit significant antifungal activity against various plant pathogenic fungi.

The antifungal mechanisms of these plant extracts are diverse and primarily involve the following three pathways: (i) disruption of cell wall integrity including *Aucklandia lappa*, *Camellia sinensis*, *Phytolacca tetramera*, and *Plinia cauliflora* (Curto et al., 2021), inhibition the activity of chitin synthase and $\beta$-(1,3)-D-glucan synthase, thereby blocking the synthesis of chitin and glucan. This reduces the structural stability of the fungal cell wall, increases permeability, and enhances susceptibility to environmental stressors (Beauvais and Latgé, 2018; Gow and Lenardon, 2022). (ii) Plant extracts can target fungal cell membrane and damage its structure and function. For example, zedoary turmeric oil severely damages the cell membrane of *Phytophthora capsici* (Wang et al., 2019), leading to leakage of intracellular contents. This results in increased relative conductivity, elevated malondialdehyde (MDA) concentrations, and accumulation of glycerol, ultimately destabilizing the intracellular environment and inhibiting fungal growth. (iii) Plant-derived compounds disrupt energy metabolism pathways in pathogens. Proteomic studies revealed that potato glycoalkaloids inhibit the growth of *Fusarium solani* by interfering with mitochondrial energy metabolism (Zhang C. et al., 2023). These compounds are significantly enriched in key pathways such as pentose and glucuronate interconversion, propanoate metabolism, N-glycan biosynthesis, pentose phosphate pathway, and carbon fixation in photosynthetic organisms, thereby obstructing energy production and limiting fungal proliferation. However, research on the antifungal activity and antifungal mechanism of plant extracts against pathogens of tea gray blight disease is limited.

This study evaluated the antifungal activity of 11 plant extracts against *N. ellipsospora* of tea gray blight disease and systematically examined the impacts of osthole and carvacrol on the mycelial morphology, mycelial weight, cell microstructure, membrane permeability, various biochemical substrate levels and related gene expression levels of *N. ellipsospora*. The aim of this study was not only to screen the antifungal activity of 11 plant extracts against *N. ellipsospora*, but also to further explore the inhibitory mechanism of osthole and carvacrol against *N. ellipsospora*, thus providing certain theoretical support for green prevention and control of tea gray blight disease in tea gardens.

## 2 Materials and methods

### 2.1 Materials, medium and natural products

The *N. ellipsospora* test strain was isolated and identified from tea gray blight disease, provided by Guizhou Tea Research Institute. PDA (Potato Dextrose Agar Medium) and PDB (Potato Dextrose Broth) culture media were sourced from Guangdong Huankai. The leaves of Fuding Dabai tea trees were picked from the tea tree resource nursery of Guizhou Tea Research Institute. Plant extracts including citronellol, eugenol, abietic acid, geraniol, ferulic acid, myrcene, carvacrol, cinnamic acid, linalool, osthole, alpha-terpineol and citral with a purity of $\geq$97% were purchased from Shanghai Aladdin Biochemical Technology Co., Ltd. in China and stored at 4°C.

### 2.2 Mycelial growth inhibition assay

The antifungal activity of plant extracts against *N. ellipsospora* was determined by the mycelial growth rate method (Mo et al., 2021). The plant extracts were dissolved in DMSO and then diluted with sterile water containing Tween 80 to five different concentrations. They were blended with quantitative PDA (at 40–45°C) and then poured into petri dishes. After the medium solidified, a 0.6 cm diameter fungal disc of *N. ellipsospora* was placed in the center of PDA. Subsequently, the petri dishes were sealed with sealing film and incubated inversely in the dark at 28°C. The PDA without drug treatment was set as the control group (CK). When the colonies in the control group grew to two-thirds of the diameter of the petri dish, the diameter of each colony (cm) was measured by the cross method. The inhibition rate was calculated

according to formula (1), and the virulence regression equation was established to calculate the $EC_{50}$ value.

The formula for calculating the inhibition rate (I, %) is as follows:

$$I\,(\%) = 100 \times \frac{\text{Mycelial diameter of the control group} - \text{Mycelial diameter of the treatment group}}{\text{Mycelial diameter of the control group is 0.6 cm}} \quad (1)$$

## 2.3 Determination of antifungal activity on carvacrol and osthole against *N. ellipsospora*

### 2.3.1 Determination of the mycelial quantity of *N. ellipsospora*

Carvacrol and osthole solutions were added respectively into the quantitative PDA and mixed evenly to make the final concentrations of carvacrol and osthole in PDA reach their $EC_{50}$ values. The medium was poured into petri dishes. After the medium cooled, a sterile cellophane (Beijing Solabio Technology Co., Ltd., Beijing, China) was placed on the surface of the PDA medium. Then a 0.6 cm diameter *N. ellipsospora* colony was placed in the center of medium, sealed, and incubated in the dark at 28°C for 7 d. Then the mycelia were collected and weighed.

### 2.3.2 Evaluation of the indoor effectiveness

Referring to Zhang's research (Zhang J. et al., 2024), the alteration of *N. ellipsospora*'s infectivity on semi-*in vitro* tea leaves under carvacrol and osthole treatment was investigated. Tea leaves with uniform size and tenderness were harvested from Fuding Dabai tea trees for experiment. These leaves were rinsed with distilled water to eliminate surface dust, sterilized with 75% alcohol solution, and then air-dried for subsequent application. Four spots were selected on each leaf and punctured with a sterile needle (three tea leaves are set in each treatment group), ensuring the wound area was less than 0.6 $cm^2$. Subsequently, a 0.6 cm diameter *N. ellipsospora* colony was positioned on each wound. The carvacrol and osthole solutions at $EC_{50}$ concentration was evenly sprayed with sterile water serving as control. The leaves were then incubated in a culture chamber at 28°C and 80% relative humidity for 7 d (only water is provided for each tea leaf). Then the lesion area on the leaves was observed, photographed, and measured using Image J software. The relative inhibition rate was computed according to Formula (2).

$$\text{Relative inhibitionrate}(\%) = \frac{\text{Disease spot area in the control group} - \text{Disease spot area in the treated group}}{\text{Disease spot area in the control group}} \quad (2)$$

### 2.3.3 Indirect effects of carvacrol on mycelial growth

The indirect activity of carvacrol against *N. ellipsospora* was determined with reference to the research method of Zhang (Zhang J. et al., 2024). Carvacrol was dissolved in DMSO and then diluted with sterile water containing Tween 80 to five concentration gradients of 4, 8, 16, 32, and 64 μL/mL for standby. PDA was poured into petri dishes, with 15 mL in each plate. After the medium solidified, colonies were inoculated and the plates were inverted. Then, 1.5 mL of the prepared reagent was evenly spread in the center of the lid of petri dish, and the dishes were quickly sealed with sealing film. The plates were incubated in the dark at 28°C for 6 d. The group without drug treatment was used as the control, and the inhibition rate was calculated as described in Section 2.2.

## 2.4 Observation of mycelial morphology by optical microscopy

According to Section 2.3.1, the drug-containing medium was prepared and poured into plates. After the medium cooled down, the *N. ellipsospora* colonies were placed in the center of medium, and then placed a sterile coverslip around the colony. Subsequently, it was incubated in the dark at 28°C and observed the morphological changes of mycelia under an optical microscope (Olympus BX53, Japan) at 24, 48, 72, 96, and 120 h, respectively.

## 2.5 Mycelial morphology and ultrastructure of mycelial cells

According to Section 2.3.1, the mycelia obtained and cultured for 72 h, washed with PBS three times, and then fixed with 2.5% glutaraldehyde at 4°C for 12 h.

SEM (Wang et al., 2023) (Scanning Electron Microscopy): poured out the fixative solution, washed the mycelia with ultrapure water three times, with each wash lasting 10 min. After post-fixing with 1% osmium tetroxide for 1–2 h, washed it with ultrapure water three times again, each time for 10 min. Then dehydrated it with alcohol step by step with a concentration gradient of 30%−50%−70%−90%−100% (change the 100% concentration three times), each time for 15 min. Put the fungus into a critical point dryer for drying, attached the fungus to the sample stage with conductive adhesive, and then put it into an ion sputtering coater (Smart Coater, Japan) for gold sputtering treatment. Observed it under a scanning electron microscope (JSM-IT700HR, Japan) and collect images.

TEM (Zhang C. et al., 2023) (Transmission Electron Microscopy): fixation: the samples were pre-fixed in 2.5% glutaraldehyde and then post-fixed in 1% osmium tetroxide. Dehydration: acetone was used for stepwise dehydration, with the concentration gradient of the dehydrating agent being 30%−50%−70%−80%−90%−95%−100% (the 100% concentration was replaced three times). Infiltration: The dehydrating agent and Epon - 812 embedding medium were infiltrated successively according to the ratios of 3:1, 1:1, and 1:3. Embedding: the samples were embedded with pure Epon - 812 embedding medium. Ultrathin Sectioning: Ultrathin sections of 60–90 nm were prepared using an ultramicrotome and collected on copper grids. Staining: staining was carried out at room temperature. First, the sections were stained with uranyl acetate for

10–15 min, and then with lead citrate for 1–2 min. After drying, the slices were observed using TEM (JEOL, JEM-1400FLASH, Japan).

## 2.6 CFW

Calcofluor white (Li et al., 2020) (CFW) stain can bind to chitin and glucan in the cell walls of fungi and emit blue fluorescence. The changes in cell wall structure can be observed through fluorescence intensity. Obtained mycelia treated for 72 h according to Section 2.3.1. Mixed the obtained mycelia with 5 μL of HEPENGBIO staining solution (Hepeng, Shanghai, China), and incubated them for 5 min under dark conditions at room temperature. After incubation, rinsed the mycelia with 500 μL of HEPENGBIO washing solution, repeating the rinsing process 2 to 3 times. Finally, placed 10 μL of mycelia suspension on a glass slide and observed it under a fluorescence microscope (Olympus BX51, Japan) with an excitation wavelength of 355 nm and an emission wavelength of 440 nm.

## 2.7 PI

Propidium iodide (Ma et al., 2025) (PI) stain can penetrate the cell membrane and release red fluorescence when binding to double-stranded DNA when the cell membrane is damaged. Therefore, it can be used to judge the damage situation of the cell membrane. Obtained mycelia treated for 72 h according to Section 2.3.1. Placed the obtained mycelia in 0.5 mL of PI stain with a concentration of 20 mg/L and incubated them for 20 min. Then washed them with PBS buffer solution, prepared slides, and observed them under a fluorescence microscope (Olympus BX51, Japan) with an excitation wavelength of 535 nm.

## 2.8 Detection of the integrity of mycelial cell membranes

### 2.8.1 Determination of relative electrical conductivity

Electrical conductivity is one of the key indicators for evaluating the balance of cell membrane permeability (Mutlu-Ingok and Karbancioglu-Guler, 2017). Three 0.6 cm diameter *N. ellipsospora* fungal cakes were placed in PDB and cultured for 72 h under the conditions of 28°C and 160 rpm. Then the mycelia were collected and washed three times with PBS. Subsequently, 0.1 g of mycelia were weighed and placed into 30 mL of sterile water (CK), osthole aqueous solution and carvacrol aqueous solution respectively. The electrical conductivity of each sample at 0, 30, 90, 120, 150, 180, 210 and 240 min was measured using a DDS-319L conductivity meter (Leici Shanghai, China), and the electrical conductivity measured at each time point was recorded as R0. After 240 min, the samples were placed in a boiling water bath and heated for 10 min. After cooling, the electrical conductivity measured at this time was the absolute electrical conductivity (R1). Finally, the relative electrical conductivity at each time point was calculated according to the following formula (3):

$$\text{Relative electrical conductivity (\%)} = (R0)/(R1) \times 100 \quad (3)$$

### 2.8.2 Measurement of extracellular nucleic acid and protein contents

The mycelia were obtained and treated in accordance with Section 2.8.1. The supernatants of each group of solutions were collected at 0, 30, 90, 120, 150, 180, 210 and 240 min respectively. The absorbance (OD value) of supernatants at 260 nm (nucleic acid) and 280 nm (protein) was measured using a microplate reader (Zhang C. et al., 2023). Meanwhile, the absorbance of the osthole solution and carvacrol solution without bacteria as well as the sterile water in the control group at 260 nm and 280 nm was measured to remove the background values of the solutions.

## 2.9 Determination of enzyme activities related to the cell wall of mycelia

### 2.9.1 Determination of chitinase activity

Three *N. ellipsospora* disc with a diameter of 0.6 cm were placed in Potato Dextrose Broth (PDB) medium. After being cultured for 72 h, osthole and carvacrol were added. After continuous culturing for 24, 48, 72, 96, and 120 h, the mycelia were taken out, washed with distilled water for three times, filtered for 10 min, and then 0.1 g of mycelia was obtained. It was quickly frozen in liquid nitrogen and then placed in a refrigerator at −80°C for later use. The standard curve of chitinase was drawn according to the chitinase assay kit (Solarbio Science & Technology Co., Ltd., Beijing, China), and the enzyme activity was determined.

Specific operation: place 0.1 g of mycelia in 1 mL of the extraction solution and carry out homogenization in an ice bath. Subsequently, centrifuge at 10,000 g at 4°C for 20 min and collect the supernatant. Add Reagent 1, Reagent 2, Reagent 3 and Reagent 4 in the kit, mix them thoroughly and then incubate at 37°C for 20 min. Finally, aspirate 200 μL of the reaction solution into a 96-well plate, measure the absorbance at 540 nm, and calculate the chitinase activity accordingly.

### 2.9.2 Determination of β-1,3-glucanase activity

The mycelia were obtained according to the method in Section 2.9.1. About 0.1 g of mycelia were weighed, quickly frozen in liquid nitrogen, and then placed in a refrigerator at −80°C for later use. The standard curve of $\beta$-1,3-glucanase was drawn according to the $\beta$-1,3-glucanase assay kit (Solabio Technology Co., Ltd., Beijing), and the activity of $\beta$-1,3-glucanase in the mycelia was determined.

Specific operation: place 0.1 g of mycelia in 1 mL of the extraction solution and conduct homogenization in an ice bath. Subsequently, centrifuge at 10,000 g at 4°C for 10 min and collect the supernatant. Add Reagent 1 and Reagent 2 in the kit, mix them thoroughly, then heat in boiling water for 5 min, cool with running water. Finally, aspirate 200 μL of the reaction solution into a 96-well plate, measure the absorbance at 540 nm, and calculate the activity of $\beta$-1,3-glucanase accordingly.

TABLE 1 qRT-PCR primers designed for chitinase and $\beta$-1,3-glucanase related genes.

| Gene ID | Symbol | Forward primer | Reverse primer | Length of the qPCR product (bp) |
|---|---|---|---|---|
| Unigene0003399 | – | AGGATACCAAGACACCATCTCA | TACCAGTACAGACTAGCGTTGA | 168 |
| Unigene0003516 | CHI-1 | AGACGGTCATTGGATACTACGA | GCAGTGTTGATGTGGCTCAC | 106 |
| Unigene0005261 | – | AATATCCTACAACAGCCAATGC | CAATGCCGCAGTGCTTCT | 119 |
| Unigene0005918 | CHIA | ACTTCCTCTCGCACTATGGTT | ATGTAGCCTTCGGCATCAGTA | 100 |
| Unigene0005921 | CHIA | AGATGACGGAATATGCTGACTT | CTCGGTGAGGTTGGTATGC | 116 |
| Unigene0006229 | CHIT33 | CGGTGCGACTTATACTGAAGG | TTGGCGGTTGCTGTGTTG | 102 |
| Unigene0006638 | – | CGAATGGCTGTCCGATACTTG | CGAGACGAGACTGACGATGT | 130 |
| Unigene0011593 | CHIB | AACGGCTATCGCACGGTAG | CGGGTCTGACATTGGCAAAG | 124 |
| Unigene0012534 | CHIT42 | TGACACAGCCATTACCTTGATG | GCAGTAGAGACACAAAGTTGGT | 107 |
| Unigene0012535 | CHI1 | CGAGCCTATACGCCACAAAT | CAGCATAAGAGTCTGACGAGTA | 109 |
| Unigene0003517 | CHIT1 | CAGTAATCGGTGGTCCATCC | GGTCCAATCACATAGTCAGCAA | 120 |
| Unigene0005919 | – | GTCACATCAAGAAGCGAACCA | AAGCGGAACTGCGTGTCA | 109 |
| Unigene0005920 | – | ACTCGGCATCGTCACTTATTG | GGTGTCGTACTTGGCACTTAC | 113 |
| Unigene0000571 | ARB_01444 | AGATTGACCACACGACATACTT | CCAGCCTCCTTCCACTTGA | 167 |
| Unigene0000927 | XGEA | TTCTTCAAGTACCTCACCTC | TGTAAGCAGAGACGGTAAG | 118 |
| Unigene0001384 | CEL74A | ATGATTGAGTCGCTGGAGATTG | TGCCTGGATGGAGATGTTGT | 126 |
| Unigene0010833 | – | GTCCTGCGAAGGCTAGAGAAG | CGGTGCTCCTTGGATTCCTG | 113 |

## 2.10 Determination of enzyme activities related to the mycelial respiratory chain

The mycelia were obtained according to the method described in Section 2.9.1. Then, 0.05 and 0.1 g of mycelia were weighed respectively, rapidly frozen in liquid nitrogen, and then stored in a refrigerator at −80°C. Subsequently, the activities of NAD-MDH and SDH enzymes were determined using the kits produced by Beijing Company Technology Co., Ltd.

## 2.11 Detection of expression of mycelial chitinase gene and $\beta$-1,3-glucanase gene

The mycelia were cultured according to the method described in Section 2.9.1. After continuous culturing for 48 h, it was washed with distilled water for three times and filtered for 10 min. Subsequently, the total RNA for qRT-PCR analysis was extracted using the RNAprep Pure Plant Kit (Tiangen, Beijing, China), and the yield and quality of the total RNA were evaluated. Then, cDNA synthesis was carried out according to the kit produced by Tiangen. Then PCR was conducted on a 96-well plate via the SYBR Green method and the Bio-Rad CFX96 qRT-PCR system (Bio-Rad, Berkeley, CA, USA), with 3 biological replicates for each sample. The final reaction volume was 20 μL, including 0.8 μL of cDNA template, 10 μL of 2×SuperReal PreMix Plus (Tiangen, Beijing, China), 0.6 μL of forward primer (200 nM), 0.6 μL of reverse primer (200 nM) (Table 1, with glyceraldehyde-3-phosphate dehydrogenase gene (GAPDH) as the internal reference, F: AGGAGCATCTTCTGTTGACCAT, R: GGACCTCTGCGTGTATAAGTTG), and 8 μL of RNase-free dd$H_20$. The reaction conditions included denaturation at 95°C for 1 min, followed by 40 cycles of denaturation at 95°C for 10 s, annealing at 60°C for 30 s. Finally, the relative gene expression levels were quantified by the $2^{-\Delta\Delta Ct}$ method.

## 2.12 Statistical analysis

All the experiments were conducted at least three times, and the results were presented as the means ± standard errors. Significant differences among the groups were assessed via one-way analysis of variance with Tukey's honest significant difference (HSD) test. $P < 0.05$ was considered as statistically significant. Statistical analyses were carried out with SPSS version 24.0. All figures were generated with the Origin 2021 software package.

# 3 Results

## 3.1 Inhibitory effect of plant extracts on mycelial growth of *N. ellipsospora*

The results were shown in Table 2. All 11 plant extracts exhibited certain antifungal activities. The $EC_{50}$ values of most plant extracts were below 100 mg/L. Among them, carvacrol and osthole had the best antifungal effects on *N. ellipsospora* among them, with $EC_{50}$ values of 9.38 and 24.40 mg/L, respectively. Therefore, we would further explore the antifungal mechanism

TABLE 2 The $EC_{50}$ values of different plant extracts against *N. ellipsospora*.

| Natural compound | Regression equation | $EC_{50}$ (mg/L) | $R^2$ | 95% confidence interval (mg/L) |
|---|---|---|---|---|
| Citronellol | $y = -4.4975x + 4.5242$ | 125.69 | 0.981 1 | 115.58–136.68 |
| Eugenol | $y = 1.8082x + 1.7864$ | 61.20 | 0.972 7 | 46.62–80.33 |
| Abietic acid | $y = 1.9681x + 1.6203$ | 74.33 | 0.950 3 | 50.92–108.52 |
| Geraniol | $y = 0.2924x + 2.4067$ | 90.37 | 0.990 3 | 79.70–102.47 |
| Ferulic acid | $y = 1.236x + 2.1774$ | 53.54 | 0.892 3 | 27.52–104.16 |
| Myrcene | $y = 2.2549 + 1.5737x$ | 55.50 | 0.992 9 | 47.55–64.79 |
| Carvacrol | $y = 2.762x + 1.613$ | 24.40 | 0.956 9 | 16.92–35.21 |
| Cinnamic acid | $y = 2.3582x + 0.9604$ | 563.44 | 0.872 3 | 206.76–840.61 |
| Linalool | $y = 3.7114x + 0.9187$ | 25.28 | 0.959 0 | 11.73–54.46 |
| Osthole | $y = 3.3599x + 1.6873$ | 9.38 | 0.980 0 | 7.62–11.54 |
| Alpha-Terpineol | $y = 1.0762x + 1.9253$ | 109.15 | 0.911 5 | 60.76–196.08 |
| Citral | $y = 2.3927x + 0.9997$ | 46.97 | 0.952 1 | 36.35–60.70 |

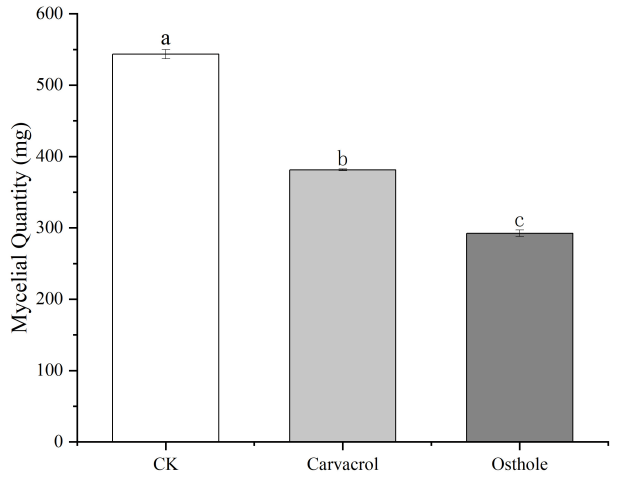


FIGURE 1
Effect of carvacrol and osthole on the mycelial quantity of *N. ellipsospora*. Different lowercase letters indicate a statistically significant difference at $P < 0.05$.

of carvacrol and osthole against *N. ellipsospora* at their $EC_{50}$ concentrations in follow-up studies.

## 3.2 Antifungal activity of carvacrol and osthole on *N. ellipsospora*

### 3.2.1 Effect of carvacrol and osthole on the mycelial quantity of *N. ellipsospora*

The results were shown in Figure 1. After 6 d of cultivation, the mycelial weight of the groups treated with carvacrol and osthole were 381.33 mg and 292.30 mg, respectively, while the mycelia weights of control group was 543.43 mg. Compared with control group, the amounts of mycelia treated with carvacrol and osthole decreased by 29.83 and 46.21% with significant differences, respectively. They could effectively inhibit the accumulation of the mycelia quantity in *N. ellipsospora*.

### 3.2.2 Indoor control effect of carvacrol and osthole on tea gray blight

To further clarify the antifungal activities of carvacrol and osthole, we explored the changes in the ability of tea gray blight to infect tea leaves under the influence of carvacrol and osthole by observing the lesion areas on the leaves. The results were shown in Figure 2. Obvious lesions appeared on the tea leaves in control group, and the lesion areas were relatively large. Although lesions still emerged on the leaves treated with carvacrol and osthole, their lesion areas were significantly reduced compared to those of control group. By calculating the relative inhibition rates, the relative inhibition rates of carvacrol and osthole were 80.85 and 74.87%, respectively (Figure 3).

### 3.2.3 Indirect effects of carvacrol on mycelial growth

Carvacrol belongs to essential oil compounds. In order to comprehensively understand its antifungal activity, we explored the indirect activity of carvacrol. The results were shown in Figure 4 and Table 3. Among the five concentration gradients we set, the inhibition rates ranged from 16.67 to 74.36%, and the $EC_{50}$ value was 20.57 μL/mL, indicating good non-contact antifungal activity.

## 3.3 Effect of carvacrol and osthole on the mycelial morphology of *N. ellipsospora*

To study the effects of osthole and carvacrol on the mycelial morphology of *N. ellipsospora*, we observed the mycelial

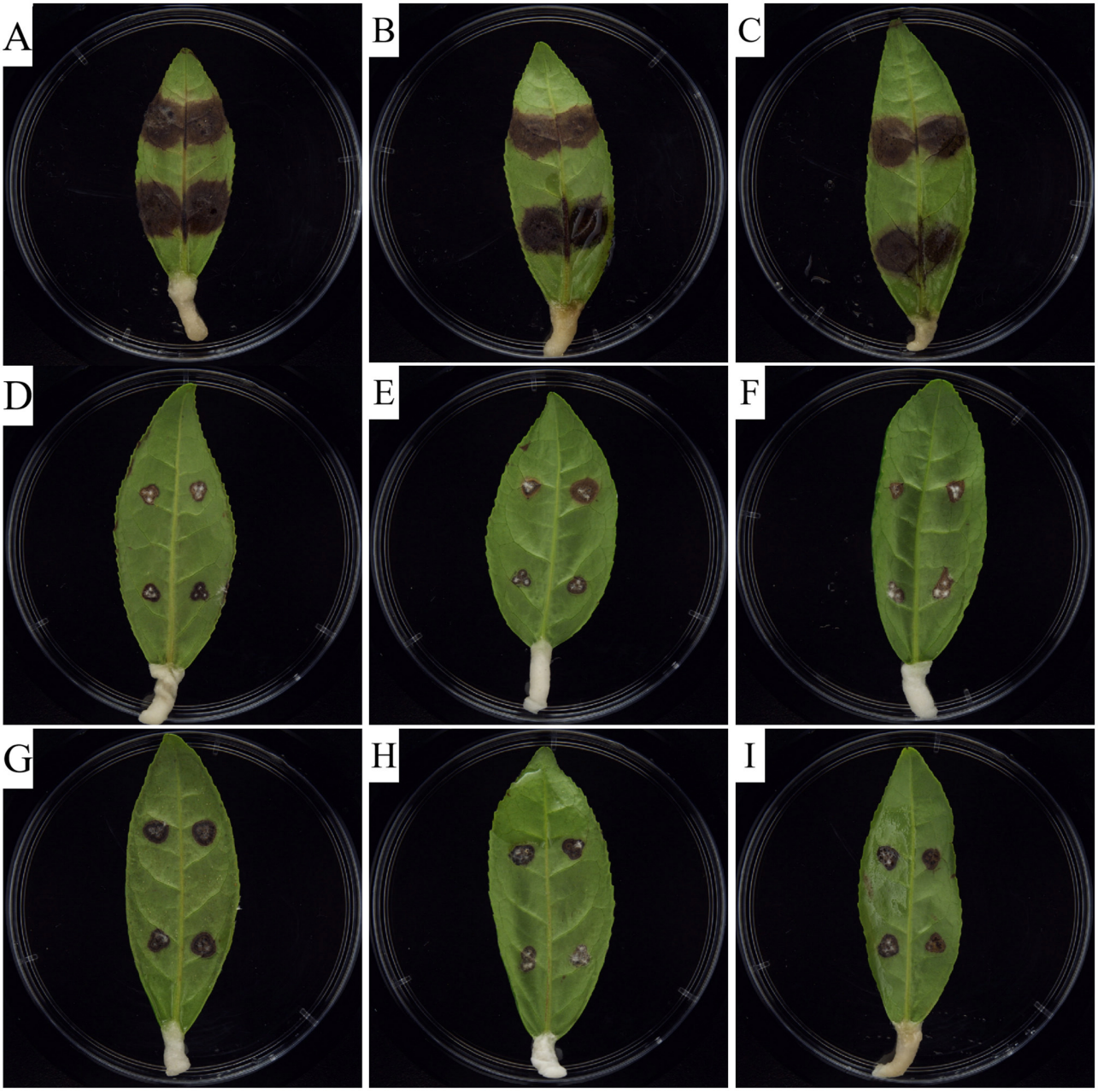


FIGURE 2
Indoor control effect of carvacrol and osthole on tea gray blight. **(A–C)** CK (0 mg/L), **(D–F)** Carvacrol ($EC_{50}$), **(G–I)** Osthole ($EC_{50}$).

morphology at different times after treatment with osthole and carvacrol for 24, 48, 72, 96, and 120 h. The results were shown in the Figure 5. The mycelial structure in the control group appeared to be intact, plump, and smooth (Figure 5A, D, G, J and M). However, the mycelia treated with carvacrol and osthole showed varying degrees of damage (Figure 5). The growing tips of the mycelia were abnormally enlarged and invaginated, the thickness of the mycelia in the middle was uneven, and the intracellular contents were reduced. These indicated that osthole and carvacrol might be affected the normal growth of the mycelia in *N. ellipsospora*.

## 3.4 Effect of carvacrol and osthole on mycelial morphology and ultrastructure in *N. ellipsospora*

### 3.4.1 SEM observation

As shown in the Figures 6A–C, the surface of mycelia in control group was smooth, without obvious damage or deformation, and it was in a good growth state. The mycelia treated with carvacrol and osthole became wrinkled, twisted and collapsed. In addition, abnormal swelling occurred in parts of mycelia in

osthole-treated group. These results indicated that both carvacrol and osthole could have a negative impact on the growth of mycelia.

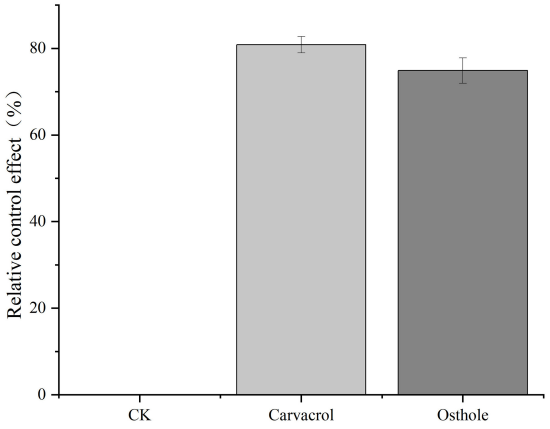


FIGURE 3
Effects of different carvacrol and osthole on tea gray blight.

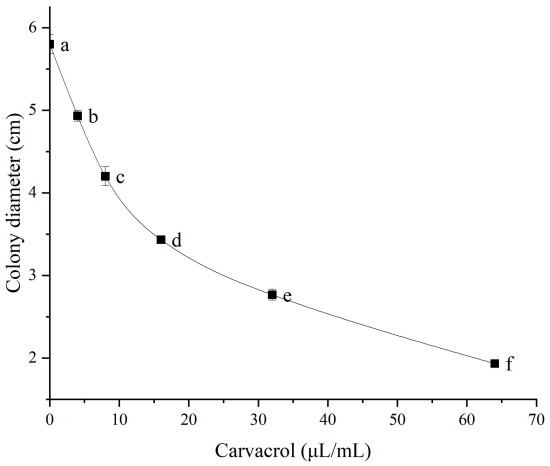


FIGURE 4
Indirect determination of antifungal activity. Different lowercase letters indicate a statistically significant difference at $P < 0.05$.

### 3.4.2 TEM observation

Transmission electron microscopy was used to observe the effects of carvacrol and osthole on the ultrastructure of *N. ellipsospora*. The calculation results were shown in Figure 6. In control group (Figures 6D, G), the cytoplasm of mycelial cells was abundant, the cell walls were of uniform thickness, the cell membranes were wavy, and the organelles were in normal morphology. In treatment groups (Figures 6E, H, F, I), the cell walls were distorted, the cell membranes shrank inward, the organelles inside the cells were arranged in a disorderly manner, and some organelles seemed to have been dissolved or damaged. These indicated that carvacrol and osthole might have adverse effects on cell structure of *N. ellipsospora*.

## 3.5 CFW

We observed the effects of carvacrol and osthole on the cell walls of *N. ellipsospora* through the intensity of blue fluorescence. The results were shown in Figure 7A. In control group (Figures 7A:a,d), strong and bright blue fluorescence appeared at the nodes and edges of the mycelia. For the mycelia treated with carvacrol (Figures 7A:b,e), the nodes still had bright blue fluorescence. However, the fluorescence intensity at the edges of mycelia was significantly weakened. In osthole-treated group (Figures 7A:c,f), the fluorescence intensity at both the nodes and edges of mycelia was also significantly reduced. These indicated that carvacrol and osthole could disrupted the dynamic balance of cell walls in *N. ellipsospora*.

## 3.6 PI

When the cell membrane is damaged, it can bind to nucleic acids and emit red fluorescence; otherwise, it cannot. The results were shown in Figure 7B. There were no obvious areas with enhanced staining in either control group or treatment groups, indicating that under the treatment with osthole and carvacrol, the cell membranes of mycelia still maintained relatively good integrity and the PI dye could not enter the cells.

TABLE 3 The indirect antifungal activity of different concentrations of carvacrol against *N. ellipsospora*.

| Carvacrol concentration (μL/mL) | Inhibition rate (%) | Regression equation | $EC_{50}$ (μL/mL) | $R^2$ |
|---|---|---|---|---|
| 0 | 0 | $y = 3.2738 + 1.3143x$ | 20.57 | 0.9984 |
| 4 | 16.67 | | | |
| 8 | 30.77 | | | |
| 16 | 45.51 | | | |
| 32 | 58.33 | | | |
| 64 | 74.36 | | | |

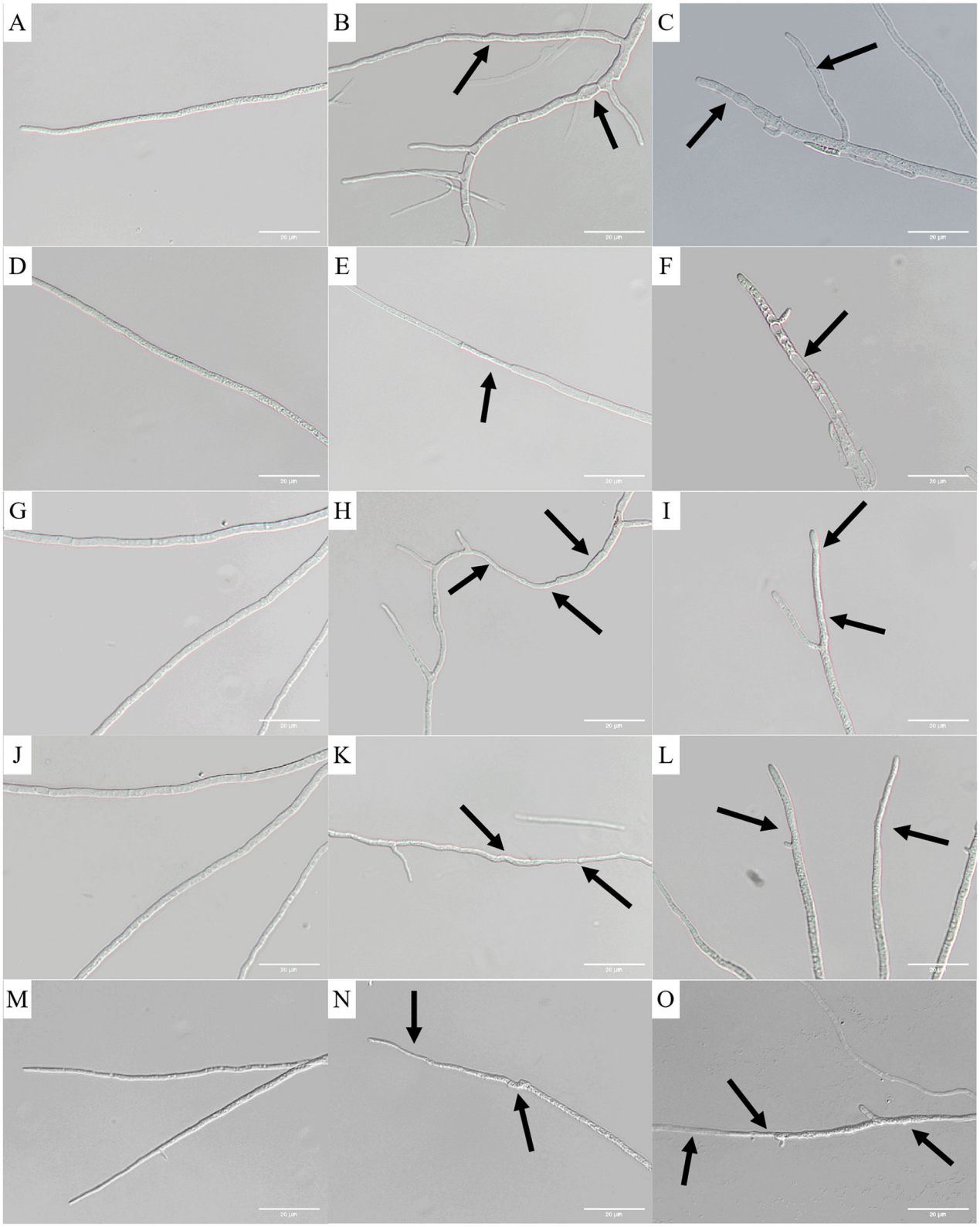


FIGURE 5
Effects of carvacrol and osthole on morphology of *N. ellipsospora*. 24 h: **(A)** CK, **(B)** carvacrol, **(C)** osthole; 48 h: **(D)** CK, **(E)** Carvacrol, **(F)** Osthole; 72 h: **(G)** CK, **(H)** Carvacrol, **(I)** Osthole; 96 h: **(J)** CK, **(K)** Carvacrol, **(L)** Osthole; 120 h: **(M)** CK, **(N)** carvacrol, **(O)** osthole. The scale bar is 20 μm.

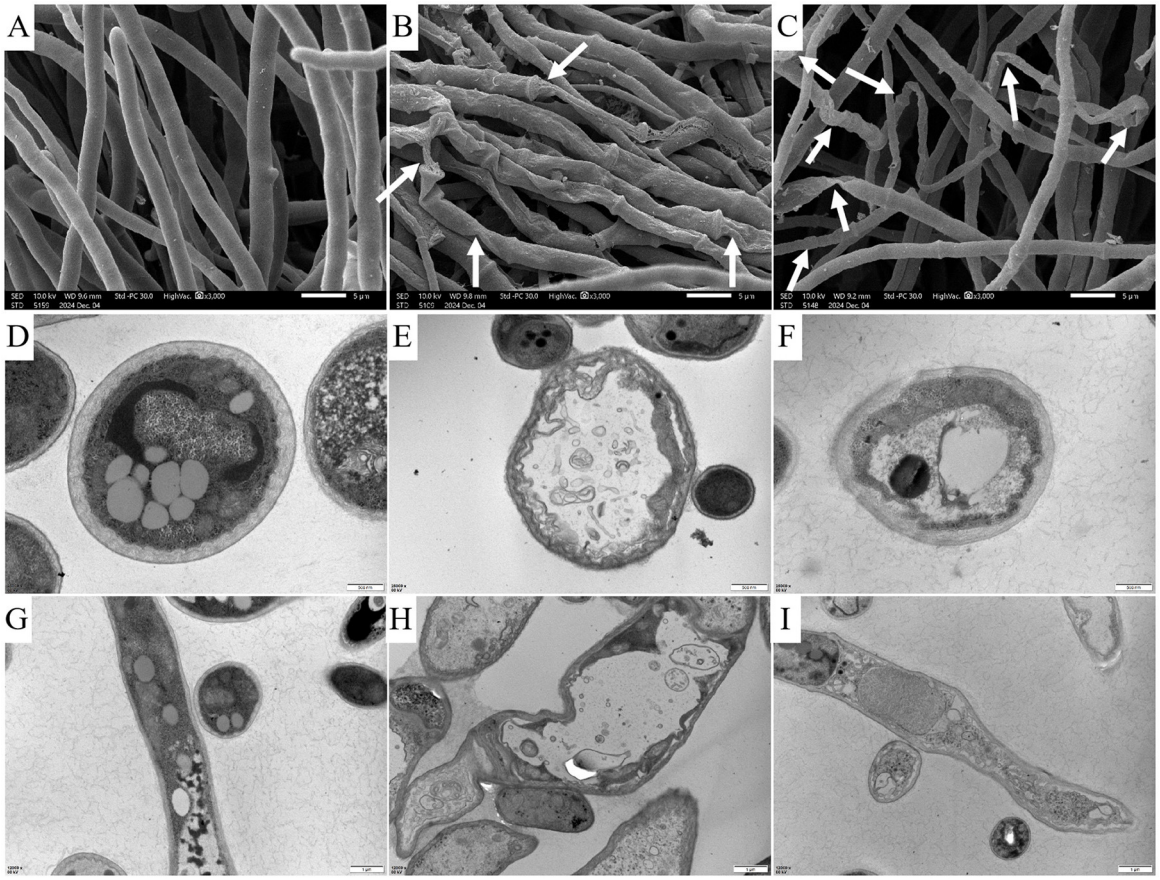


FIGURE 6
Images of changes in the mycelial surface and cellular ultrastructure after treatment with carvacrol and osthole for 72 h. SEM: **(A)** CK, **(B)** Carvacrol, **(C)** osthole. The scale bar is 5 μm. TEM of cross - sections of cells: **(D)** CK, **(E)** Carvacrol, **(F)** Osthole. The scale bar is 500 nm. TEM of longitudinal sections of cells: **(G)** CK, **(H)** Carvacrol, **(I)** Osthole. The scale bar is 1 μm.

## 3.7 Effect of carvacrol and osthole on cell membrane of *N. ellipsospora*

### 3.7.1 Effects of carvacrol and osthole on membrane permeability of *N. ellipsospora*

The cell membrane serves as a barrier between the cell and the external environment and can strictly control the entry and exit of substances such as ions. Therefore, the change in cell membrane permeability can be reflected by measuring the electrical conductivity of mycelia. The results were shown in the Figure 8. As time increases, the relative electrical conductivity of the mycelia in both control group and treated groups also increases. While the trends of relative electrical conductivity in mycelia treated with osthole and carvacrol were the same as that of the mycelia in the control group, with no significant differences.

### 3.7.2 Effect of carvacrol and ostholee on the release of cell components in *N. ellipsospora*

Nucleic acids are the main carriers of biological genetic information, and proteins are essential components of life. The leakage of nucleic acids and proteins can lead to programmed disorders in cellular activities and is one of the important indicators reflecting damage to the cell membrane. Through detection, it was found that, the contents of nucleic acids and proteins in the supernatants of each group increased to varying extents during 0–240 min. Among them, there were no significant differences in the contents of nucleic acids and proteins between osthole-treated group and control group (Figures 9A,B). However, the contents of nucleic acids and proteins in supernatant after carvacrol treatment were slightly higher than those in control group. Specifically, the protein content increased rapidly within 60 min, then the growth rate slowed down, and the protein content increased rapidly again after 180 min. There was a significant difference in protein content at 240 min compared with that of control group. The analysis results indicated that carvacrol might damage the cell membrane of *N. ellipsospora*, while osthole had no obvious effect on it.

## 3.8 Effect of carvacrol and osthole on cell wall-associated enzyme activity in *N. ellipsospora*

### 3.8.1 Effect of carvacrol and osthole on chitinase activity in *N. ellipsospora*

Chitin (Plaza et al., 2019) is the main component of the cell walls of most fungi, which can provide strength and

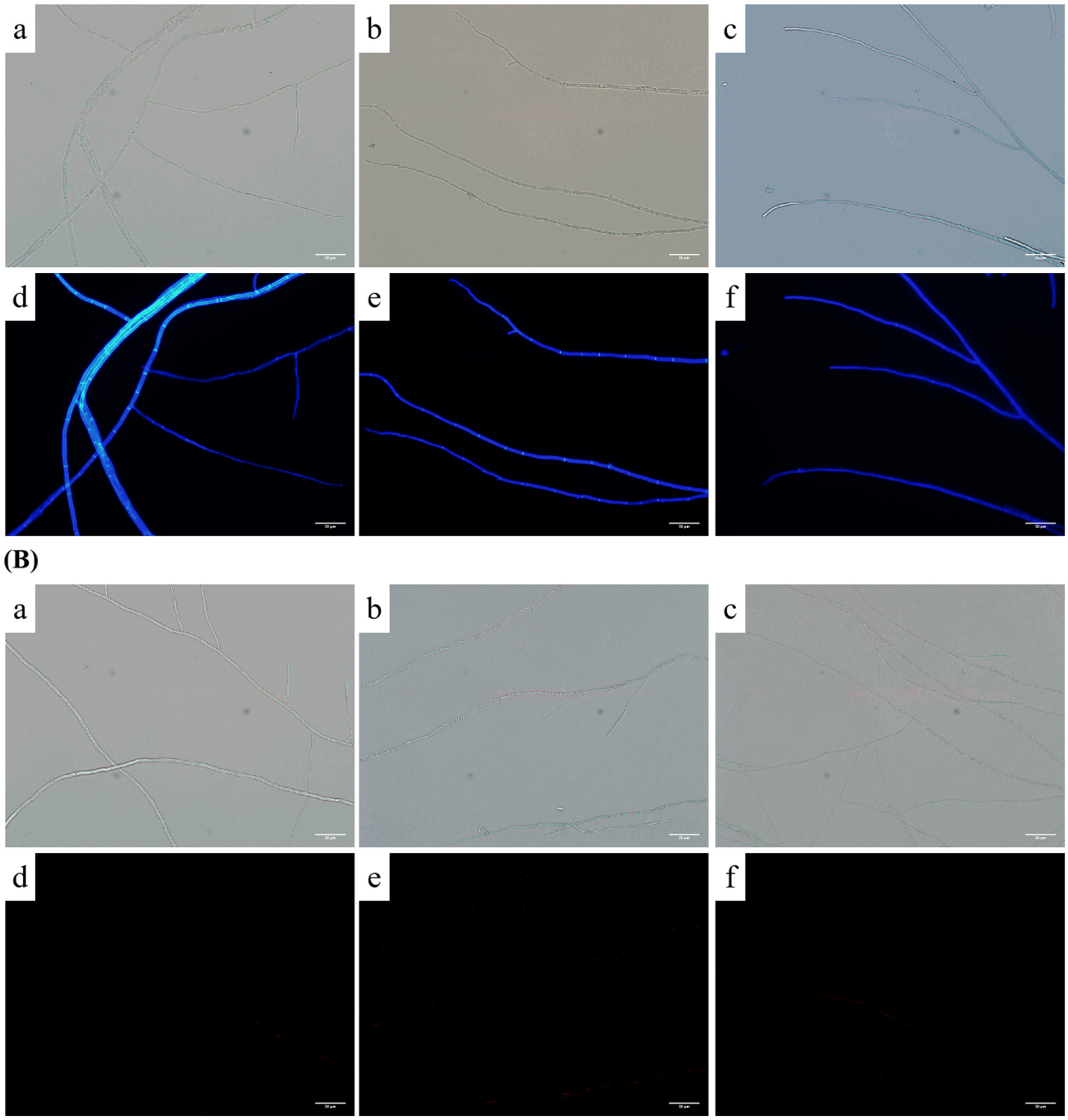


FIGURE 7
CFW and PI fluorescence effect of mycelia after treatment with carvacrol and osthole for 72 h. **(A)** CFW fluorescence: (a, d) CK; (b, e) Carvacrol, (c, f) Osthole. **(B)** PI fluorescence: (a, d) CK; (b, e) Carvacrol, (c, f) Osthole. The scale bar is 20 μm.

stability to the cell walls. Chitinase can catalyze the hydrolysis of chitin and is an important indicator for judging the integrity of cell walls. As shown in the standard curve (Figure 10A), there was a good linear relationship between the concentration of chitinase and the absorption peak area, and the regression equation was $y = 0.0012x + 0.0079$, $R^2 = 0.9980$. After being treated with osthole and carvacrol (Figure 10C), the activity of chitinase was significantly higher than that of control group at 48 h, being 2.35 times and 1.87 times that of control group, respectively. Subsequently, it decreased at 72 h time point, while the chitinase activity of osthole increased again at 96 h, reaching 2.12 times that of control group. The results indicated that osthole and carvacrol could enhance the chitinase activity of *N. ellipsospora*.

### 3.8.2 Effect of carvacrol and osthole on β-1,3-glucanase activity in *N. ellipsospora*

Glucan (Fang et al., 2023) is an important component of cell walls, and $\beta$-1,3-glucanase can catalyze its hydrolysis. With the concentration of $\beta$-1,3-glucanase as the abscissa and the absorbance value as the ordinate, a standard curve y = 1.1523x-0.0519 was obtained, with $R^2 = 0.9979$ (Figure 10B). Within 24–120 h (Figure 10D), the activities of glucanase in both control group and treatment groups increased. At 24 h, there was no significant difference between control group and treatment groups. Differences began to emerge at 48 h. At 72 h, the enzyme activities in treatment groups were lower than those in control group. The enzyme activities of osthole and carvacrol were 3.39 and 4.45 U/g, respectively. At 96 h, both of them were also lower than those in control group. These results indicated that osthole and carvacrol had an inhibitory effect on $\beta$-1,3-glucanase of *N. ellipsospora*.

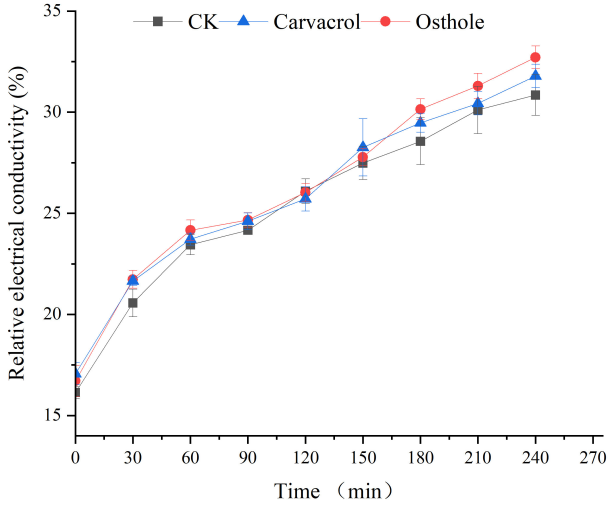


FIGURE 8
Effect of carvacrol and osthole on membrane permeability of *N. ellipsospora*.

## 3.9 Effect of carvacrol and osthole on SDH and NAD-MDH enzyme activity in *N. ellipsospora*

SDH and NAD-MDH are important indicators for evaluating mitochondrial respiratory metabolism (Mo et al., 2021). The Figure 11 showed that when *N. ellipsospora* was treated with carvacrol within 120 h, the activity of NAD-MDH was increased and higher than that of control group from 0 to 72 h, then decreases after 72 h, and was lower than that of the control group at 96 h. While the change trend of SDH activity was similar and significantly higher than that of control group at multiple time points, indicating that carvacrol increased the SDH and NAD-MDH enzyme activities of *N. ellipsospora*. After treatment with osthole, the SDH and NAD-MDH enzyme activities of the mycelia were higher than those of control group before 72 h, and lower than those of tcontrol group after 72 h, and the change trend was the same as that of control group.

## 3.10 Effect of osthole and carvacrol on the expression of cell wall-associated enzyme activity in *N. ellipsospora*

To further verify the effects of carvacrol and osthole on the cell wall of *N. ellipsospora*, we assessed their impact by measuring changes in the expression of chitinase and $\beta$-1,3-glucanase genes. Based on the transcriptome data previously obtained by our research group, we selected 18 related genes (including GAPDH) for qRT-PCR analysis.

Chitinase gene expression analysis (Figure 12A): After 48 h of carvacrol treatment, the expression levels of genes regulating chitinase were significantly higher than those in control group. Specifically, the expression levels of eight genes - Unigene0003399, Unigene0003516, Unigene0005261, Unigene0005921, Unigene0006638, Unigene0011593, Unigene0003517, and Unigene0005920 - were significantly upregulated, reaching 2.31-fold, 2.14-fold, 3.85-fold, 2.88-fold, 1.69-fold, 2.87-fold, 2.86-fold, and 4.37-fold of control group, respectively. In contrast, the effect of osthole on chitinase genes was relatively weaker. Although a large number of genes showed upregulated expression, the differences were not statistically significant. These results indicated that both carvacrol and osthole could promote the expression of chitinase genes in *N. ellipsospora*, and the gene expression levels were consistent with changes in enzyme activity.

$\beta$-1,3-Glucanase gene expression analysis (Figure 12B): In carvacrol treatment group, the expression levels of $\beta$-1,3-glucanase genes Unigene0000571 and Unigene0010833 in *N. ellipsospora* were significantly upregulated, reaching 4.98-fold and 2.76-fold of control group, respectively, while the expression of Unigene0000927 was downregulated by 91.00%. In osthole treatment group, the expression levels of Unigene0000927 and Unigene0010833 were downregulated to 64.68% and 71.58% of control group, respectively, while the expression of Unigene0001384 was upregulated to 1.66-fold of control group.

In summary, both carvacrol and osthole significantly regulated the expression of cell wall-related genes in *N. ellipsospora*, with carvacrol showing a more pronounced promoting effect on the expression of chitinase and $\beta$-1,3-glucanase genes.

# 4 Discussion

Tea, one of the world's three major non-alcoholic beverages, holds great economic significance (Chang et al., 2023). The young leaves and buds of tea plants are highly valuable, but tea leaf diseases burden tea planting and raise costs. For example, the tea gray blight can cut production by 10–20% (Murugavel et al., 2024). Currently, chemical control dominates in tea—growing areas. While it curbs diseases, it causes severe issues (Rani et al., 2020; Sookhtanlou et al., 2021; Zhang Z. et al., 2023) like pesticide residues, endangering tea quality, consumer health, and reducing international market competitiveness. Thus, exploring eco—friendly, safe, and efficient plant disease control methods is imperative.

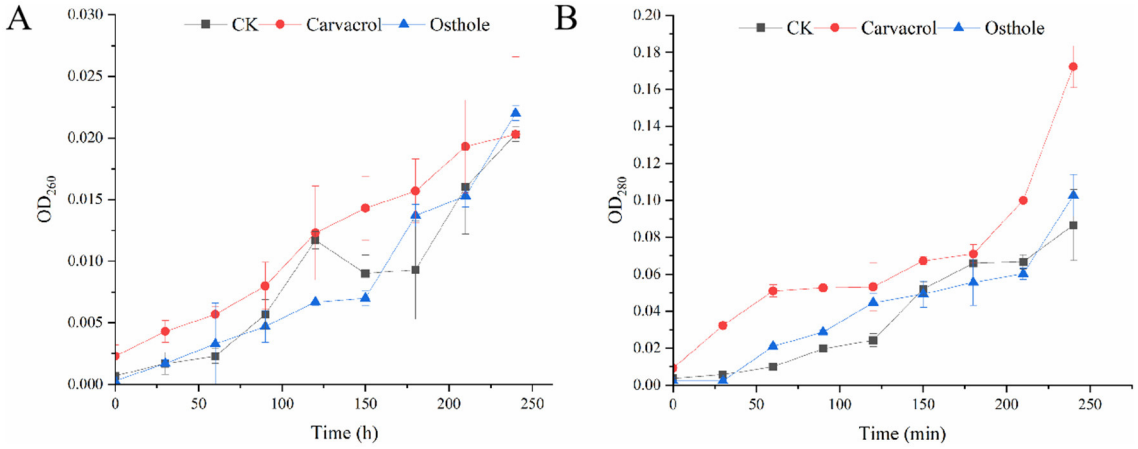


FIGURE 9
Effect of carvacrol and ostholee on the release of cell components in *N. ellipsospora*: **(A)** nucleic acid leakage, **(B)** protein leakage.

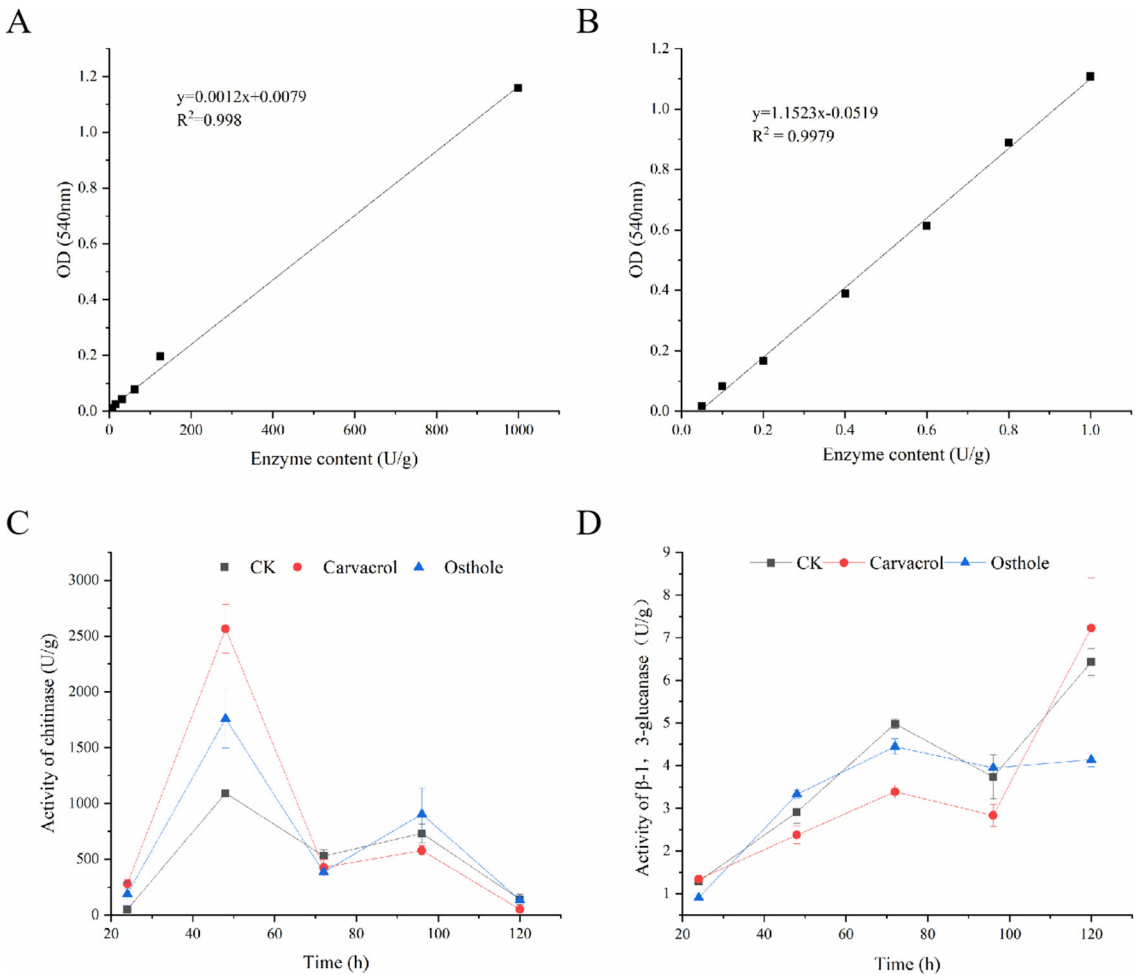


FIGURE 10
Enzyme activity of mycelia in *N. ellipsospora* treated with osthole and carvacrol. Standard curves of chitinase **(A)** and $\beta$-1,3-glucanase **(B)**. Chitinase activity **(C)** and $\beta$-1,3-glucanase activity **(D)**.

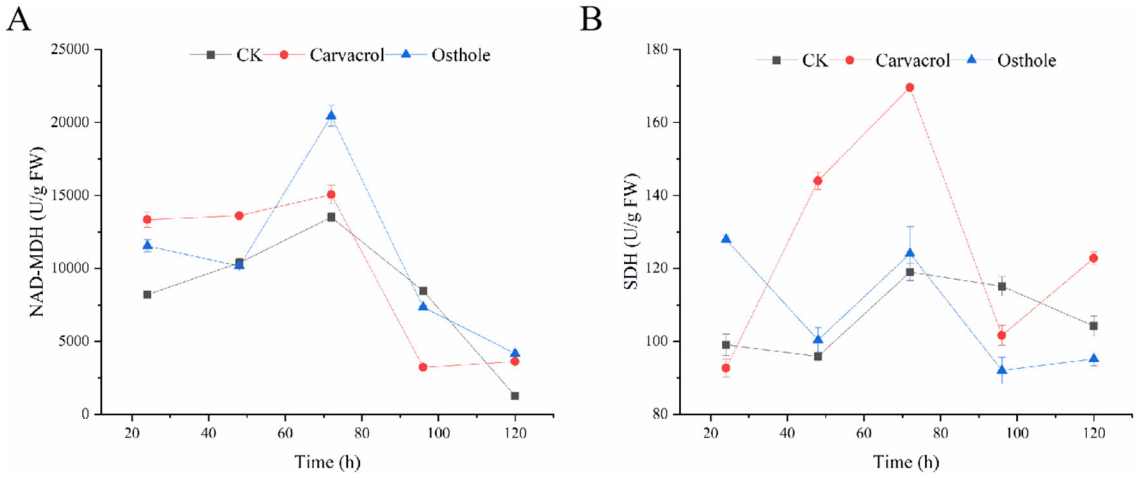


FIGURE 11
Effects of osthole and carvacrol on energy metabolism of *N. ellipsospora*. **(A)** Effect of osthole and carvacrol on NAD-malate dehydrogenase (NAD-MDH) activity. **(B)** Effect of osthole and carvacrol on succinate dehydrogenase (SDH) activity.

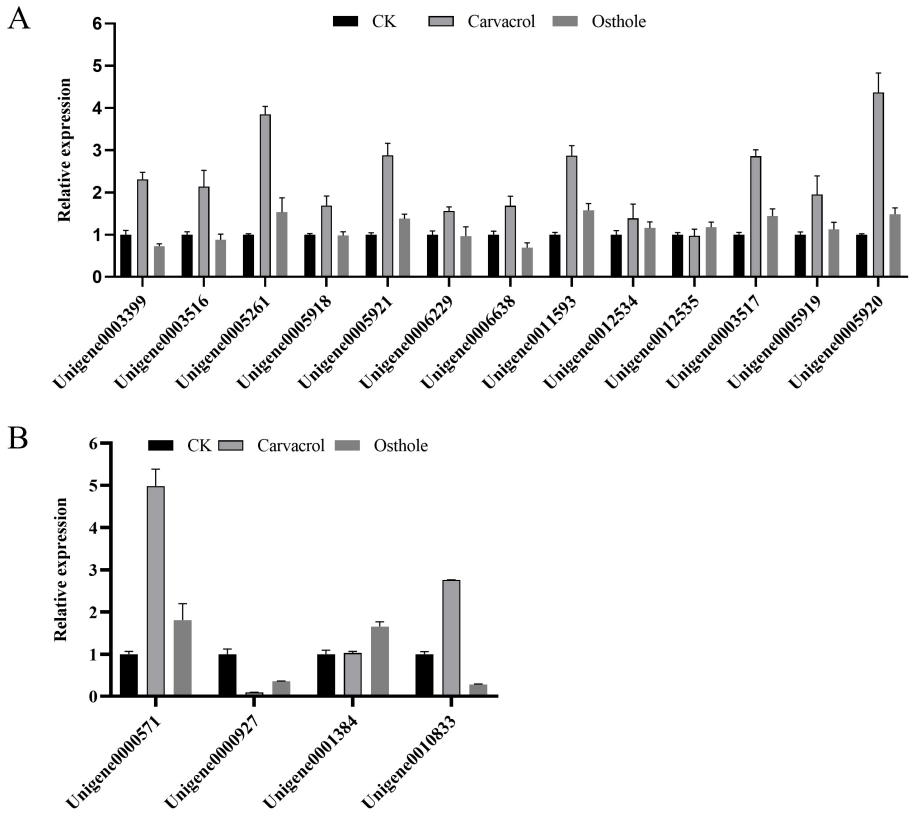


FIGURE 12
**(A)** Effects of osthole and carvacrol on the expression of chitinase genes; **(B)** Effects of osthole and carvacrol on the expression of $\beta$-1,3-glucanase genes. Error bars denote standard error of the mean for three independent experiments.

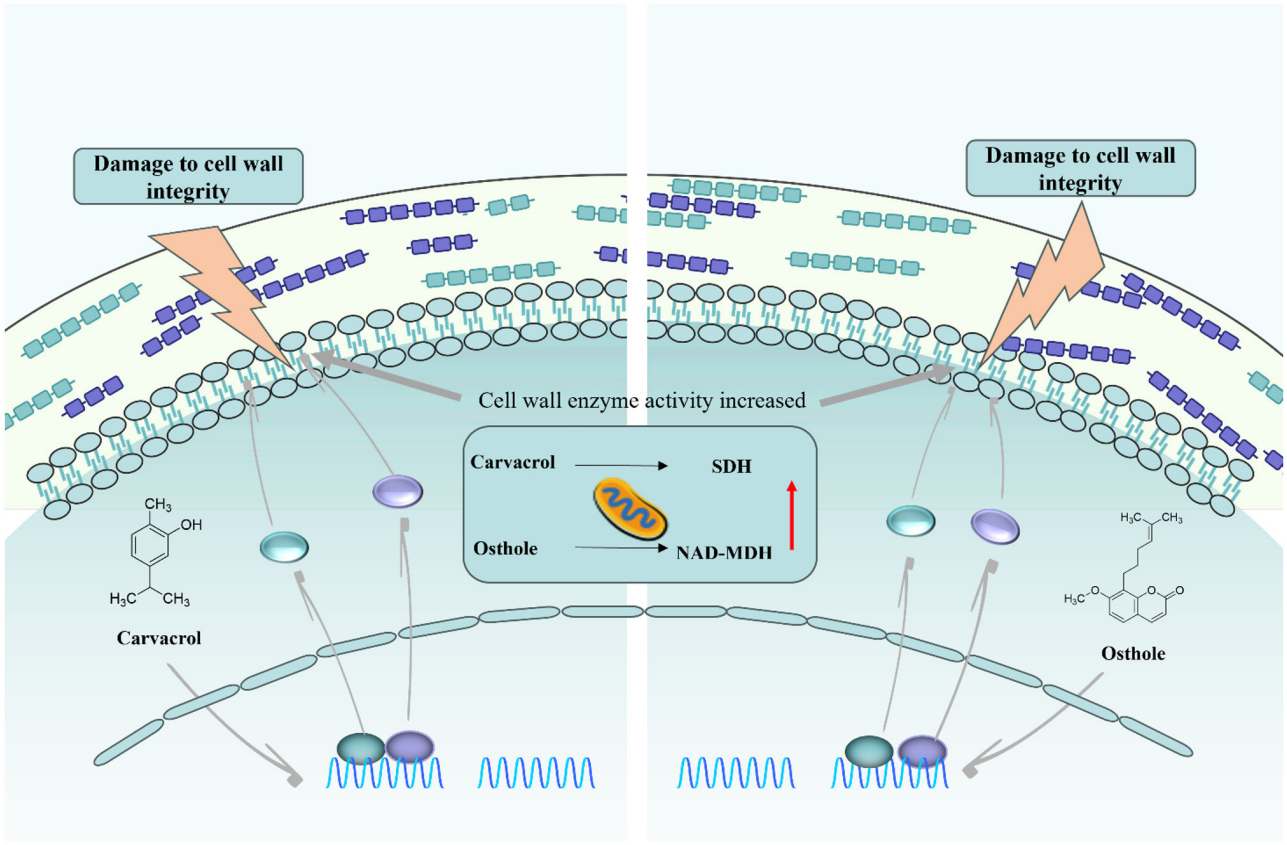


FIGURE 13
Schematic diagram of the mechanism of action of carvacrol and osthole against *N. ellipsospora*.

Plant extracts have attracted extensive attention as one of the ideal alternatives to chemical pesticides due to their safe, green, and efficient characteristics (Chemat et al., 2019). In this study, the antifungal activities of 11 plant extracts against the tea gray blight pathogen *N. ellipsospora* were screened. The results showed that all 11 plant extracts exhibited good antifungal activities, with $EC_{50}$ values ranging from 9.38 to 563.44 mg/L. Among them, carvacrol, an essential oil extract, performed the best, with an $EC_{50}$ of 24.40 mg/L, and its $EC_{50}$ for indirect contact was 20.57 μL/mL. This characteristic enables carvacrol to effectively inhibited the accumulation of pathogen mycelia and significantly reduced the incidence of tea gray blight on tea leaves, showing great potential in the control of tea plant diseases.

Observation under an optical microscope revealed that the mycelia treated with carvacrol and osthole showed abnormal enlargement and invagination, and these results were corroborated by the observation results of a scanning electron microscope. Further observation with a transmission electron microscope showed that the cell walls, cell membranes, and organelles of the treatment groups were damaged to varying degrees, indicating that the cell wall and membrane were likely to be the key targets for the antifungal effects of carvacrol and osthole. To explore the action mechanisms of these two substances more deeply, we used multiple methods such as PI staining, relative conductivity measurement, and extracellular nucleic acid and protein detection. The results showed that the cell membrane could still maintain a relatively intact state at the $EC_{50}$ concentration. Combined with the CFW staining results, it was clear that carvacrol and osthole mainly acted on the cell wall and damaged the integrity of cell wall of *N. ellipsospora*.

The cell walls of most fungi are mainly composed of chitin and $\beta$-glucan (Arroyo et al., 2016). Chitin, as a nitrogen-containing polysaccharide, forms a fibrous structure in the fungal cell wall, providing the necessary strength and toughness (Qinghui et al., 2024) for the cell wall and helping fungal cells maintain a specific shape and structural stability. $\beta$-glucan forms a reticular structure, giving the cell wall rigidity, enabling the cell to resist external pressure and having a certain elasticity to buffer external impacts (Osumi, 1998). Chitinase and glucanase (Adams, 2004) can respectively decompose chitin and glucan in the cell wall. Once their enzyme activities change abnormally, the dynamic balance of the cell wall will be disrupted, and then the integrity of the cell wall will be damaged. Under the action of carvacrol and osthole, the chitinase activity of the cell wall showed a trend of first increasing and then decreasing. It had a significant difference compared with control group at 48 h, and then decreased to a level close to that of control group at 72 h. This phenomenon might be the self-regulation of the mycelium in response to external stimuli (Ayling et al., 2000; Rui-Feng et al., 2021). In contrast, the activity of $\beta$-1,3-glucanase was inhibited at different times, and this change in enzyme activity disrupted the normal structure and function of cell wall.

To further reveal their molecular mechanisms of action, we found through qRT-PCR analysis that carvacrol and osthole had the same trend of influence on the expression levels of chitinase and $\beta$-1,3-glucanase-related genes at 48 h. This result indicated that these two substances not only affected the synthesis and decomposition of the cell wall at the enzyme activity level, but also regulated it at the gene expression level, disrupting the integrity of the cell wall from multiple levels.

According to existing research reports, carvacrol and osthole can not only damage the cell membranes and cell walls of fungi (Ayling et al., 2000; Hu et al., 2023; Rui-Feng et al., 2021), but also some studies have shown that carvacrol can interfere with the energy metabolism balance of mycelia (Barbosa et al., 2019). Based on this, this study further explored the effects of carvacrol and osthole on the enzyme activities of SDH (succinate dehydrogenase) and NAD-MDH (malate dehydrogenase). The experimental results showed that, carvacrol caused the activity of NAD-MDH to first increase within 120 h and then decreased. Its activity was higher than that of control group from 0–72 h, started to decline after 72 h, and was lower than that of control group at 96 h. The activity of SDH also changed accordingly and was higher than that of control group at multiple time points. After treatment with osthole, the enzyme activities of SDH and NAD-MDH in mycelia were higher than those of control group before 72 h and lower than those of control group after 72 h. These results fully demonstrated that carvacrol and osthole could interfere with the normal respiratory metabolism process of *N. ellipsospora*, and inhibit the growth and reproduction of pathogens from the perspective of energy metabolism (Figure 13).

## 5 Conclusion

In conclusion, this study comprehensively and deeply explored the antifungal activities and action mechanisms of carvacrol and osthole against the tea gray blight pathogen *N. ellipsospora*, clarified the important roles of carvacrol and osthole in inhibiting the growth of pathogens, and provided a solid theoretical basis and rich experimental foundation for the development of new plant-derived fungicides. However, the current research results were still at the laboratory stage. In practical agricultural production applications, their control effects and safety would still need to be further verified through field tests. Future research could focus on in-depth exploration of their molecular mechanisms of action, such as clarifying the specific interaction methods between carvacrol, osthole and related genes and proteins, and studying their synergistic effects when used in combination with other substances, so as to provide more powerful support for better applying them to the control of diseases in agricultural production and promoting the green and sustainable development of the tea industry.

## Data availability statement

The original contributions presented in the study are included in the article/supplementary material, further inquiries can be directed to the corresponding authors.

## Author contributions

HL: Conceptualization, Data curation, Formal analysis, Funding acquisition, Investigation, Methodology, Project administration, Resources, Software, Supervision, Validation, Visualization, Writing – original draft. JY: Conceptualization, Data curation, Investigation, Software, Supervision, Validation, Writing – review & editing. RY: Conceptualization, Data curation, Investigation, Methodology, Visualization, Writing – review & editing. CM: Data curation, Formal analysis, Investigation, Methodology, Validation, Writing – review & editing. LL: Methodology, Supervision, Formal analysis, Investigation, Visualization, Software, Writing – review & editing. WY: Data curation, Formal analysis, Funding acquisition, Investigation, Methodology, Project administration, Resources, Supervision, Visualization, Writing – review & editing. ZL: Conceptualization, Data curation, Funding acquisition, Investigation, Methodology, Project administration, Resources, Software, Supervision, Validation, Visualization, Writing – review & editing.

## Funding

The author(s) declare that financial support was received for the research and/or publication of this article. This study was supported by Guizhou Provincial Basic Research Program (Natural Science No. Qiankehe foundation [2022]224); Natural Science Foundation of Guizhou Province (zk[2021]032).

## Acknowledgments

All individuals included in this section have consented to the acknowledgment.

## Conflict of interest

The authors declare that the research was conducted in the absence of any commercial or financial relationships that could be construed as a potential conflict of interest.

## Generative AI statement

The author(s) declare that no Gen AI was used in the creation of this manuscript.

## Publisher's note

# References


Adams, D. J. (2004). Fungal cell wall chitinases and glucanases. *Microbiology* 150, 2029–2035. doi: 10.1099/mic.0.26980-0

Aguilar-Rodríguez, S., López-Villafranco, M. E., Jácquez-Ríos, M. P., Hernández-Delgado, C. T., Mata-Pimentel, M. F., Estrella-Parra, E. A., et al. (2022). Chemical profile, antimicrobial activity, and leaf anatomy of Adenophyllum porophyllum var. *cancellatum*. *Front Pharmacol*. 13:981959. doi: 10.3389/fphar.2022.981959

Al-Otibi, F., Moria, G. A., Alharbi, R. I., Yassin, M. T., and Al-Askar, A. A. (2023). The antifungal properties of *Tamarix aphylla* extract against some plant pathogenic fungi. *Microorganisms* 11:127. doi: 10.3390/microorganisms11010127

Alshehri, S. A., Wahab, S., Abullais, S. S., Das, G., Hani, U., Ahmad, W., et al. (2022). Pharmacological efficacy of *Tamarix aphylla*: a comprehensive review. *Plants* 11:118. doi: 10.3390/plants11010118

Arroyo, J., Farkaš, V., Sanz, A. B., and Cabib, E. (2016). 'Strengthening the fungal cell wall through chitin-glucan cross-links: effects on morphogenesis and cell integrity. *Cell Microbiol*. 18, 1239–1250. doi: 10.1111/cmi.12615

Ayling, S. M., Smith, S. E., and Smith, F. A. (2000). Transmembrane electric potential difference of germ tubes of arbuscular mycorrhizal fungi responds to external stimuli. *New Phytol*. 147, 631–639. doi: 10.1046/j.1469-8137.2000.00723.x

Bang, K. H., Kim, Y. K., Min, B. S., Na, M. K., Rhee, Y. H., Lee, J. P., et al. (2000). Antifungal activity of magnolol and honokiol. *Arch. Pharm. Res*. 23, 46–49. doi: 10.1007/BF02976465

Barbosa, L. N., Alves, F. C. B., Andrade, B. F. M. T., Albano, M., Rall, V. L. M., Fernandes, A. A. H., et al. L.D., et al. (2019). Proteomic analysis and antibacterial resistance mechanisms of *Salmonella enteritidis* submitted to the inhibitory effect of *Origanum vulgare* essential oil, thymol and carvacrol. *J. Proteomics*. 214:103625. doi: 10.1016/j.jprot.2019.103625

Beauvais, A., and Latgé, J. (2018). Special issue: fungal cell wall. *J. Fungi*. 4:91. doi: 10.3390/jof4030091

Chang, M., Ma, J., Sun, Y., Fu, M., Liu, L., Chen, Q., et al. (2023). Role of endophytic bacteria in the remobilization of leaf nitrogen Mediated by CsEGGT in tea plants (*Camellia sinensis* L.). *J. Agr. Food Chem*. 71, 5208–5218. doi: 10.1021/acs.jafc.2c08909

Chattopadhyay, P., Banerjee, G., and Mukherjee, S. (2017). Recent trends of modern bacterial insecticides for pest control practice in integrated crop management system. *3 Biotech* 7:60. doi: 10.1007/s13205-017-0717-6

Chemat, F., Abert-Vian, M., Fabiano-Tixier, A. S., Strube, J., Uhlenbrock, L., Gunjevic, V., et al. (2019). Green extraction of natural products. Origins, current status, and future challenges. *Trac-Trend Anal. Chem*. 118, 248–263. doi: 10.1016/j.trac.2019.05.037

Chen, C., Liu, Y., Abdullah, N., Chen, H., Cao, Y., Chen, Y., et al. (2023). Antimicrobial activity of electrospun nanofibers film incorporated with momordica charantia seed oil for strawberry freshness. *Food Bioprocess Tech*. 17, 2678–2692. doi: 10.1007/s11947-023-03284-x

Chen, J., Liu, Q., and Gao, L. (2019). Visual tea leaf disease recognition using a convolutional neural network model. *Symmetry* 11:343. doi: 10.3390/sym11030343

Chu, N., Shu, X., Yuan, L., Zhang, X., Tang, M., Yang, J., et al. (2022). Determination of 52 hidden chemical pesticides in biopesticide products by GC-MS/MS and LC-MS/MS. *J. Environ. Sci. Health Part B*. 57, 504–515. doi: 10.1080/03601234.2022.2072645

Cui, C., Yang, Y., Zhao, T., Zou, K., Peng, C., Cai, H., et al. (2019). Insecticidal activity and insecticidal mechanism of total saponins from *Camellia oleifera*. *Molecules* 24:4518. doi: 10.3390/molecules24244518

Cui, J., Wu, B., and Zhou, J. (2024). Changes in amino acids, catechins and alkaloids during the storage of oolong tea and their relationship with antibacterial effect. *Sci. Rep. UK*. 14:10424. doi: 10.1038/s41598-024-60951-5

Curto, M. Á., Butassi, E., Ribas, J. C., Svetaz, L. A., and Cortés, J. C. G. (2021). Natural products targeting the synthesis of β (1,3)-D-glucan and chitin of the fungal cell wall. Existing drugs and recent findings. *Phytomedicine* 88:153556. doi: 10.1016/j.phymed.2021.153556

Fang, S., Shang, X., He, Q., Li, W., Song, X., Zhang, B., et al. (2023). A cell wall-localized β-1,3-glucanase promotes fiber cell elongation and secondary cell wall deposition. *Plant Physiol*. 194, 106–123. doi: 10.1093/plphys/kiad407

Garvey, M. (2022). Bacteriophages and food production: biocontrol and bio-preservation options for food safety. *Antibiotics* 11:1324. doi: 10.3390/antibiotics11101324

Gow, N. A. R., and Lenardon, M. D. (2022). Architecture of the dynamic fungal cell wall. *Nat. Rev. Microbiol*. 21, 248–259. doi: 10.1038/s41579-022-00796-9

Hernández-Ceja, A., Loeza-Lara, P. D., Espinosa-García, F. J., García-Rodríguez, Y. M., Medina-Medrano, J. R., Gutiérrez-Hernández, G. F., et al. (2021). In vitro antifungal activity of plant extracts on pathogenic fungi of blueberry (*Vaccinium* sp.). *Plants* 10:852. doi: 10.3390/plants10050852

Hu, K., Li, R., Mo, F., Ding, Y., Zhou, A., Guo, X., et al. (2023). Natural product osthole can significantly disrupt cell wall integrity and dynamic balance of *Fusarium oxysporum*. *Pestic Biochem. Phys*. 196:105623. doi: 10.1016/j.pestbp.2023.105623

Jiang, H., Zhang, M., Wang, D., Yu, F., Zhang, N., Song, C., et al. (2020). Analytical strategy coupled to chemometrics to differentiate *Camellia sinensis* tea types based on phenolic composition, alkaloids, and amino acids. *J. Food. Sci*. 85, 3253–3263. doi: 10.1111/1750-3841.15390

Jiying, Z., Jianmei, Y., Chiyu, M., Huifang, L., Wen, Y., Zhiwei, L., et al. (2024). Magnolol from Magnolia officinalis inhibits *Neopestalotiopsis ellipsospora* by damaging the cell membrane. *Sci. Rep. UK*. 14:24934. doi: 10.1038/s41598-024-75310-7

Lee, S. H., Oh, Y. T., Lee, D., Cho, E., Hwang, B. S., Jeon, J., et al. (2022). Large-scale screening of the plant extracts for antifungal activity against the plant pathogenic fungi. *Plant Pathol. J*. 38, 685–691. doi: 10.5423/PPJ.NT.07.2022.0098

Li, X., Feng, G., Wang, W., Yi, L., Deng, L., Zeng, K., et al. (2020). Effects of peptide C12-OOWW-NH2 on transcriptome and cell wall of the postharvest fungal pathogen *Penicillium digitatum*. *Front. Microbiol*. 11:574882. doi: 10.3389/fmicb.2020.574882

Luo, D., Ye, S., Qu, G., and Ba, L. (2024). Inhibitory effect and action mechanism of citral against black rot in pitaya fruit. *Physiol. Mol. Plant P*. 131:102275. doi: 10.1016/j.pmpp.2024.102275

Luo, Q., Luo, L., Zhao, J., Wang, Y., and Luo, H. (2023). Biological potential and mechanisms of tea's bioactive compounds: an updated review. *J. Adv. Res*. 65, 345–363. doi: 10.1016/j.jare.2023.12.004

Ma, J., Long, Y., Wang, W., Li, W., Chen, X., Wang, B., et al. (2025). Biocontrol potential of Streptomyces albidoflavus SC-3 on kiwifruit soft rot caused by *Botryosphaeria dothidea*. *Postharvest. Biol. Tec*. 222:113344. doi: 10.1016/j.postharvbio.2024.113344

Ma, K., Huang, X., and Kumar, B. A. (2016). Antifungal effect of plant extract and essential oil. *Chin J. Integr. Med*. 23, 233–239. doi: 10.1007/s11655-016-2524-z

Marchese, A., Barbieri, R., Coppo, E., Orhan, I. E., Daglia, M., Nabavi, S. F., et al. (2017). Antimicrobial activity of eugenol and essential oils containing eugenol: a mechanistic viewpoint. *Crit. Rev. Microbiol*. 43, 668–689. doi: 10.1080/1040841X.2017.1295225

Mo, F., Hu, X., Ding, Y., Li, R., Long, Y., Wu, X., et al. (2021). Naturally produced magnolol can significantly damage the plasma membrane of *Rhizoctonia solani*. *Pestic. Biochem. Phys*. 178:104942. doi: 10.1016/j.pestbp.2021.104942

Murugavel, K., Karthikeyan, G., Raveendran, M., Sendhilvel, V., Karthiba, L., Venkatesan, K., et al. (2024). Ustainable management of blister and grey blight diseases of tea using antagonistic and plant growth promoting microbes in Western Ghats of India. *Crop. Prot*. 187:106984. doi: 10.1016/j.cropro.2024.106984

Mutlu-Ingok, A., and Karbancioglu-Guler, F. (2017). Cardamom, cumin, and dill weed essential oils: chemical compositions, antimicrobial activities, and mechanisms of action against *Campylobacter* spp. *Molecules* 22:1191. doi: 10.3390/molecules22071191

Nair, J. J., and van Staden, J. (2017). Antifungal activity based studies of amaryllidaceae plant extracts. *Nat. Prod. Commun*. 12, 1953–1956. doi: 10.1177/1934578X1701201235

Nezelo, T. M., Fikile, N. M., Zakheleni, P. D., and Thilivhali, E. T. (2024). Potential use of *Argemone ochroleuca* sweet and argemone mexicana Linn as alternative pesticide: a systematic review on their biological activity and phytochemistry. *Physiol. Mol. Plant*. 136:102534. doi: 10.1016/j.pmpp.2024.102534

Osumi, M. (1998). The ultrastructure of yeast: cell wall structure and formation. *Micron* 29, 207–233. doi: 10.1016/S0968-4328(97)00072-3

Pandey, A. K., Sinniah, G. D., Babu, A., and Tanti, A. (2021). How the global tea industry copes with fungal diseases - challenges and opportunities. *Plant Dis*. 105, 1868–1879. doi: 10.1094/PDIS-09-20-1945-FE

Plaza, V., Silva-Moreno, E., and Castillo, L. (2019). Breakpoint: cell wall and glycoproteins and their crucial role in the phytopathogenic fungi infection. *Curr. Protein Pept. Sci*. 21, 227–244. doi: 10.2174/1389203720666190906165111

Qinghui, C., Malitha, C. D. W., Jayasubba, R. Y., Ankur, A., Jean-Paul, L., Ping, W., et al. (2024). Molecular architecture of chitin and chitosan-dominated cell walls in zygomycetous fungal pathogens by solid-state NMR. *Nat. Commun*. 15:8295. doi: 10.1038/s41467-024-52759-8

Ramalingam, R., Palanisamy, S., Mohanraj, A. K., Durisamy, S., and Rajasekaran, N. (2020). Chemical profiling of Momordica charantia. Seed essential oil and its antimicrobial activity. *J. Essent Oil Bear Pl*. 23, 390–396. doi: 10.1080/0972060X.2020.1741451

Rani, L., Thapa, K., Kanojia, N., Sharma, N., Singh, S., Grewal, A. S., et al. (2020). An extensive review on the consequences of chemical pesticides on human health and environment. *J. Clean Prod*. 283:124657. doi: 10.1016/j.jclepro.2020.124657

Rui-Feng, M., Ya-Xian, S., Jun-Li, G., Si-Ping, D., and Hao, D. Le Cai; Zhong-Tao, D. (2021). Interaction between *Alternaria alternata* and monoterpenoids caused by fungal self-protection. *Process Biochem*. 110, 142–150. doi: 10.1016/j.procbio.2021.08.003

Saleh, A. S., Abdul, O. N., and Masratul, H. M. (2021). Neopestalotiopsis clavispora and Pseudopestalotiopsis camelliae-sinensis causing grey blight disease of tea (*Camellia sinensis*) in Malaysia. *Eur. J. Plant Pathol.* 162, 709–724. doi: 10.1007/s10658-021-02433-2

Sanjay, R., Ponmurugan, P., and Baby, U. I. (2008). Evaluation of fungicides and biocontrol agents against grey blight disease of tea in the field. *Crop Prot.* 27, 689–694. doi: 10.1016/j.cropro.2007.09.014

Sawadogo, I., Paré, A., Kaboré, D., Montet, D., Durand, N., Bouajila, J., et al. (2022). Antifungal and Antiaflatoxinogenic effects of cymbopogon citratus, cymbopogon nardus, and cymbopogon schoenanthus essential oils alone and in combination. *J. Fungi* 8:117. doi: 10.3390/jof8020117

Sen, S., Rai, M., Das, D., Chandra, S., and Acharya, K. (2020). Blister blight a threatened problem in tea industry: a review. *J. King Saud Univ. Sci.* 32, 3265–3272. doi: 10.1016/j.jksus.2020.09.008

Sookhtanlou, M., Allahyari, M. S., and Surujlal, J. (2021). Health risk of potato farmers exposed to overuse of chemical pesticides in Iran. *Saf Health Work-KR.* 13, 23–31. doi: 10.1016/j.shaw.2021.09.004

Wang, B., Liu, F., Li, Q., Xu, S., Zhao, X., Xue, P., et al. (2019). Antifungal activity of zedoary turmeric oil against Phytophthora capsici through damaging cell membrane. *Pestic Biochem. Phys.* 159, 59–67. doi: 10.1016/j.pestbp.2019.05.014

Wang, Q. T., Cheng, Y. H., Zhuo, L., Wang, Y., Zhou, H., Hou, C. L., et al. (2022). Neopestalotiopsis longiappendiculata as the agent of grey blight disease of *Camellia* spp. *J. Phytopathol.* 170, 770–777. doi: 10.1111/jph.13139

Wang, W., He, L., Zhang, Z., Li, W., Chen, J., Chen, T., et al. (2023). Activity of the botanical compound thymol against kiwifruit rot caused by Fusarium tricinctum and the underlying mechanisms. *Pest Manag. Sci.* 79, 2493–2502. doi: 10.1002/ps.7431

Xu, G., Ying, F., Wu, H., and Tang, X. (2023). Biocontrol potential of two deep-sea microorganisms against gray blight disease of tea. *Egypt J. Biol. Pest Co.* 53:1577. doi: 10.1186/s41938-023-00701-3

Yuan, L., Yan, P., Han, W., Huang, Y., Wang, B., Zhang, J., et al. (2019). Detection of anthracnose in tea plants based on hyperspectral imaging. *Comput. Electron. Agr.* 167:105039. doi: 10.1016/j.compag.2019.105039

Zhang, C., Ding, D., Wang, B., Wang, Y., Li, N., Li, R., et al. (2023). Effect of potato glycoside alkaloids on energy metabolism of *Fusarium solani*. *J. Fungi* 9:77. doi: 10.3390/jof9070777

Zhang, J., Liu, H., Yao, J., Ma, C., Yang, W., Lei, Z., et al. (2024). Plant-derived citronellol can significantly disrupt cell wall integrity maintenance of *Colletotrichum camelliae*. *Pestic Biochem. Phys.* 204:106087. doi: 10.1016/j.pestbp.2024.106087

Zhang, Y., Wang, F., Wang, L., Zhang, L., Espley, R. V., Lin-Wang, K., et al. (2024). The response of growth and transcriptome profiles of tea grey blight disease pathogen pestalotiopsis theae to the variation of exogenous L-theanine. *Int. J. Mol. Sci.* 25:3493. doi: 10.3390/ijms25063493

Zhang, Z., Chen, T., Yin, X., Wang, W., Li, W., Chen, X., et al. (2023). Honokiol inhibits *Botryosphaeria dothidea*, the causal pathogen of kiwifruit soft rot, by targeting membrane lipid biosynthesis. *Pest Manag. Sci.* 80, 1779–1794. doi: 10.1002/ps.7910

Zhao, C., Tang, G., Cao, S., Xu, X., Gan, R., Liu, Q., et al. (2019). Phenolic profiles and antioxidant activities of 30 tea infusions from green, black, oolong, white, yellow and dark teas. *Antioxidants* 8:215. doi: 10.3390/antiox8070215

Zheng, S., Chen, R., Wang, Z., Liu, J., Cai, Y., Peng, M., et al. (2021). High-quality genome assembly of pseudopestalotiopsis theae, the pathogenic fungus causing tea gray blight. *Plant Dis.* 105, 3723–3726. doi: 10.1094/PDIS-02-21-0318-A

Zhou, A. A., Li, R. Y., Mo, F. X., Ding, Y., Li, R. T., Guo, X., et al. (2022). Natural product citronellal can significantly disturb chitin synthesis and cell wall integrity in *Magnaporthe oryzae*. *J. Fungi.* 8:1310. doi: 10.3390/jof8121310

Zhou, B., and Li, X. (2021). The monitoring of chemical pesticides pollution on ecological environment by GIS. *Environ. Technol. Inno.* 23:101506. doi: 10.1016/j.eti.2021.101506